Development of a Frequency Dependent Temporary Overvoltage (TOV) EMT Model for Gapless Metal-Oxide Surge Arresters

Dhulipala, S.P.P.; Engelbrecht, C.S.; Popov, M.; Velitsikakis, K.

Publication date
2025

Document Version
Final published version

Published in
Proceedings of the 2025 INMR World Congress

Development of a Frequency Dependent Temporary Overvoltage (TOV) EMT Model for Gapless Metal-Oxide Surge Arresters

S.P.P. Dhulipala[(1)], C.S. Engelbrecht[(1)], M. Popov[(1)], K. Velitsikakis[(2)]
Delft University of Technology[(1)], TenneT TSO[(2)]
pavanpratyush@gmail.com, kostas.velitsikakis@tennet.eu

Abstract - *This paper presents the development and validation of a frequency-dependent model for metal-oxide surge arresters operating under temporary overvoltage conditions containing harmonic content. As power systems evolve with increased cable deployment and renewable integration, harmonic resonances during switching operations create complex overvoltage stresses that traditional power-frequency models cannot adequately assess. Through systematic characterization from 10 Hz to 300 Hz, this research reveals that surge arrester resistance exhibits significant frequency dependence while capacitance remains stable. An RC network model implemented in ATP-EMTP captures this behavior through automated parameter extraction, reproducing measured characteristics within engineering-acceptable accuracy. The methodology provides a practical tool for assessing surge arrester thermal stress in modern cable-rich networks where harmonic content during temporary overvoltages becomes unavoidable.*

Keywords: surge arresters, temporary overvoltages, frequency-dependent model, harmonic resonance, EMTP-ATP, insulation coordination

1. Introduction

It is a fact that transmission System Operators (TSOs) are being challenged by the need for expanding their Extra High Voltage (EHV) and High Voltage (HV) grids to meet the demands for higher transmission capacities. The latter is the combined result of the load growth and the need for connecting significantly increased volumes of renewable energy generation projects, which is a must for meeting the national and international climate targets. Cable systems are gaining an increasing share in grid expansion projects; as an example, in the Dutch grid, TenneT TSO will install the coming years more than 4000 km of underground cables. As discussed in [1], the tendency of applying many and long cable connections in a transmission grid may result in low order harmonic resonances. System transient events might excite the harmonic resonances and this could lead to the

manifestation of Temporary Overvoltages (TOVs). These TOVs are harmonic distorted and lightly damped, as shown in Figure 1. Because of these characteristics, these TOVs and their evaluation become of significant importance for surge arresters [2].

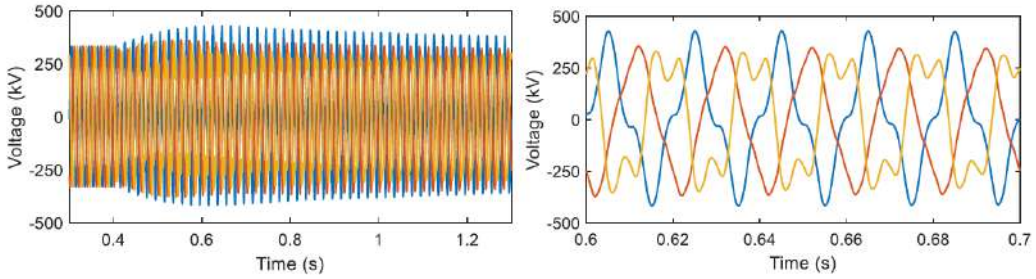

Figure 1. Example of a typical harmonic resonance TOV [1]

In general, surge arresters shall be designed and selected to protect high voltage equipment from being exposed to transient overvoltages, without being damaged by continuous voltages and TOVs. In traditional insulation coordination studies, the modelling of the surge arresters is appropriate for lightning and switching surge analysis. The arrester models are mainly based on the voltage-current characteristic and they typically represent the arrester as a nonlinear resistor [3], perhaps with parallel capacitance. Nevertheless, these models ignore the frequency-dependent behaviour. This could lead to underestimating the energy absorption of surge arresters when conducting harmonic resonance TOV studies. For this reason, a study was conducted, aiming to develop a new surge arrester modelling framework that can adequately represent the energy absorption under harmonic-rich conditions [4]. This paper presents the study findings, as a result of extended laboratory testing, and the proposed surge arrester model that was developed in EMTP-ATP.

2. Testing Methodology

A high-voltage test circuit, as seen in Figure 2, was developed to characterize surge arrester blocks across multiple frequencies. The test setup employs a precision high-voltage amplifier capable of delivering up to 30 kV at 20 mA over a frequency range extending to 300 Hz. The amplifier drives the MOV block under test through a mechanical test fixture designed to apply 1 kN of compressive force, ensuring consistent electrical contact between the block and the test electrodes. Current measurements are obtained using a 1 kΩ shunt resistor connected between the arrester's bottom electrode and ground. This configuration avoids phase distortions introduced by the amplifier's internal current monitoring. Voltage and current signals are acquired using a PicoScope 6424E oscilloscope and the sampling rates are adjusted based on test frequency.

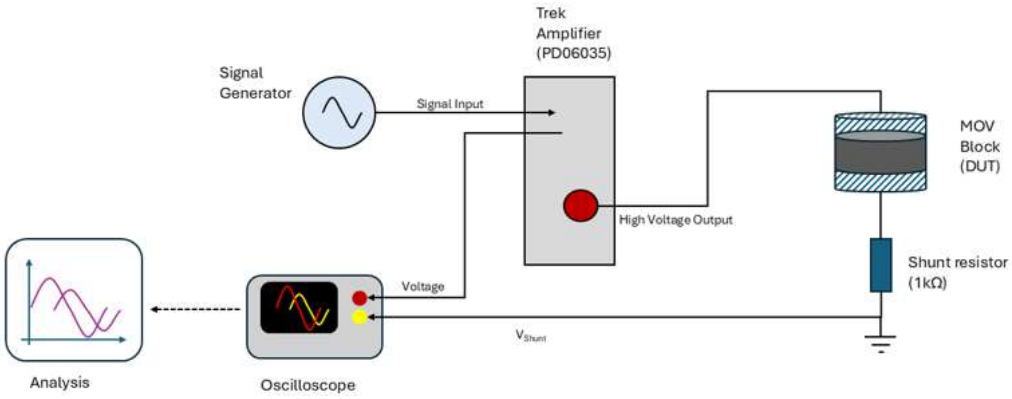

Figure 2. Single-line diagram of the test setup for frequency-dependent characterization

The validation was performed on two different station-class surge arrester blocks (Figure 3). Table 1 presents the manufacturer's specifications.

Table 1 Specifications of the MOV blocks considered in the study

Parameter	Block no.1	Block no.2
Diameter	100 mm	64.5 mm
Height	22.5 mm	44 mm
Rated voltage (rms)	3.0 kV	6.98 kV
Maximum continuous operating voltage (rms)	2.4 kV	5.48 kV
Reference voltage (rms)	4.18-4.82 kV	6.98 kV
Nominal discharge current (8/20 µs) (peak)	10 kA	20 kA
Residual voltage ratio at 10 kA	1.57	N/A
Residual voltage at 10 kA (8/20 µs) (peak)	6.56-7.57 kV	16.44 kV

Figure 3. MOV blocks (no.1 left, no.2 right) considered in the study

Measurements were conducted at frequencies of 10, 17, 27, 50, 100, 150, and 300 Hz, capturing the power frequency, harmonics up to the 6th order and sub-harmonic frequencies to cover the entire region of frequencies relevant for TOVs. Voltage levels ranged from 1.3 to 4.7 kV peak for the first block and 3.0 to 10.0 kV peak for the second

block were selected to characterize the leakage current region while maintaining measurable current levels above the noise floor of the setup. Decomposition of the measured arrester current, as seen in Figure 4, separates the total current into its capacitive and resistive components. The decomposition methodology provides insight into the distinct conduction mechanisms within the MOV structure.

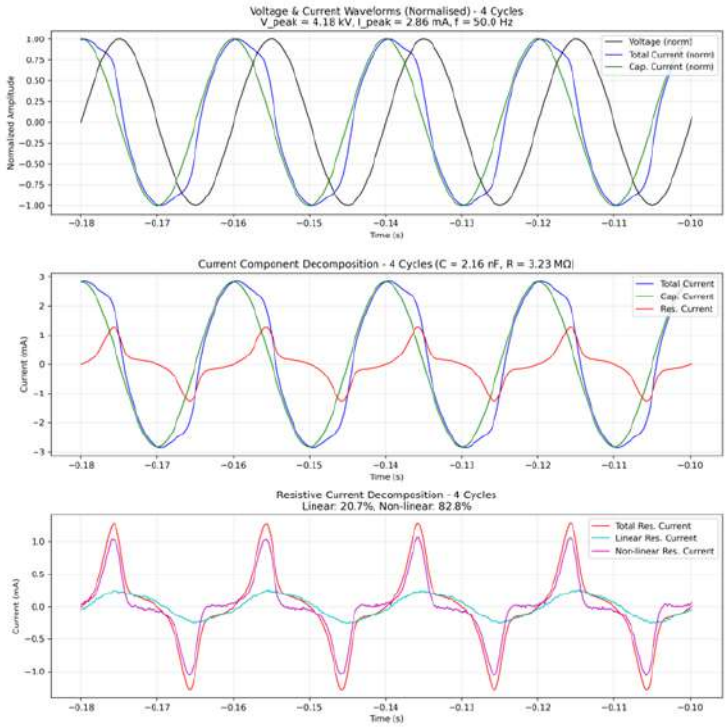

Figure 4. Current decomposition into capacitive and resistive components for block no.1 at 4.2 kV

3. Experimental Results

Figure 5 presents the extracted capacitance and resistance of block no.1 as functions of the applied voltage across the tested frequency range. The capacitance maintains a value of approximately 2.5 nF across the voltage range, demonstrating frequency independence in the pre-conduction region. This stability indicates that the geometric and material properties governing the capacitance remain unaffected by frequency variations within the tested range.

On the other hand, the resistance exhibits monotonic decrease with both voltage and frequency. At 3 kV peak, resistance decreases from approximately 10 MΩ at 10 Hz to 1 MΩ at 300 Hz. This order-of-magnitude variation demonstrates that frequency-dependent effects cannot be neglected when assessing surge arrester performance under harmonic conditions. The frequency dependence arises from dielectric relaxation processes within

the ZnO grain boundary network, where charge carriers respond to alternating fields at different time scales. The frequency-dependent resistance can be decomposed into linear and nonlinear components. The linear component, representing dielectric losses, follows a power-law relationship with frequency. The nonlinear component increases exponentially with voltage. This decomposition reveals that both frequency-dependent dielectric losses and voltage-dependent conduction contribute to the total energy dissipation in the MOV.

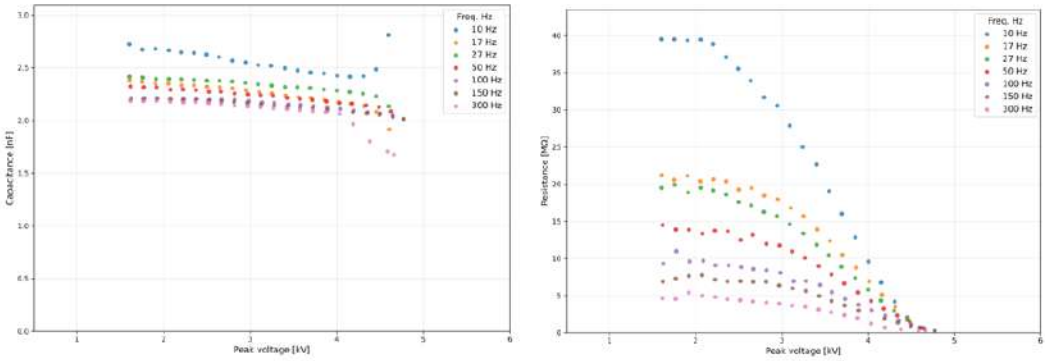

Figure 5. Extracted capacitance and resistance of the first MOV block as a function of peak applied voltage (a) Capacitance (b) Resistance

The analysis was repeated for the second block, this time up to 500 Hz. As this block has a rated voltage almost twice as that of the first block, the voltage-current characteristics are different. Nonetheless, both arrester blocks showed the same trends in terms of capacitance and resistance as seen in Figure 6. For the second block, the capacitance was approximately 0.5 nF while the resistance was frequency dependent; decreasing as the frequency increased. The anomalously high resistance values at 10 Hz for both blocks need to be investigated further. This could be attributed to initial conditioning effects in newly manufactured blocks or to inherent arrester behaviour at such low frequencies.

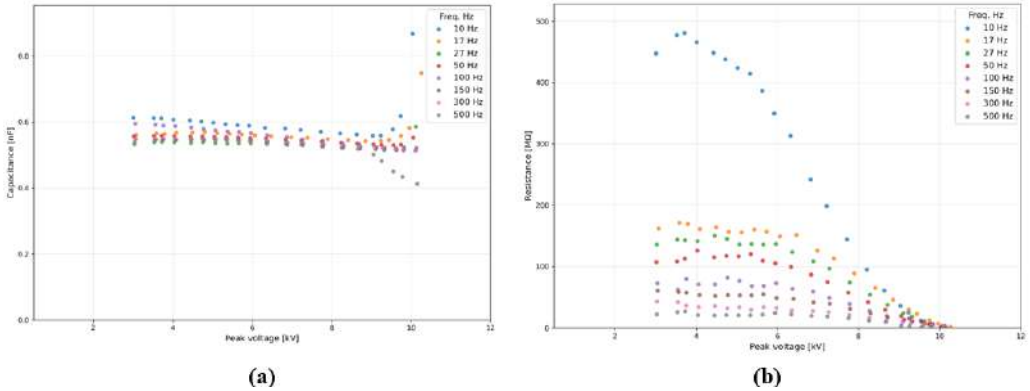

Figure 6. Extracted capacitance and resistance of the second MOV block as a function of peak applied voltage (a) Capacitance (b) Resistance

The measured voltage-current characteristics in Figure 7 reveal that below the knee voltage point of the MOV, the current is capacitive dominant while above the knee voltage, the nonlinear resistive behaviour takes over. The transition from capacitive to resistive behavior occurs between 4-4.5 kV peak for the first block and between 9–10 kV peak for the second block, corresponding to the onset of arrester conduction. For any voltage point, it is observed that as frequency increases, the current also increases, thus indicating that arresters subjected to TOV harmonics can conduct more current, which potentially could lead to thermal runway at a faster rate.

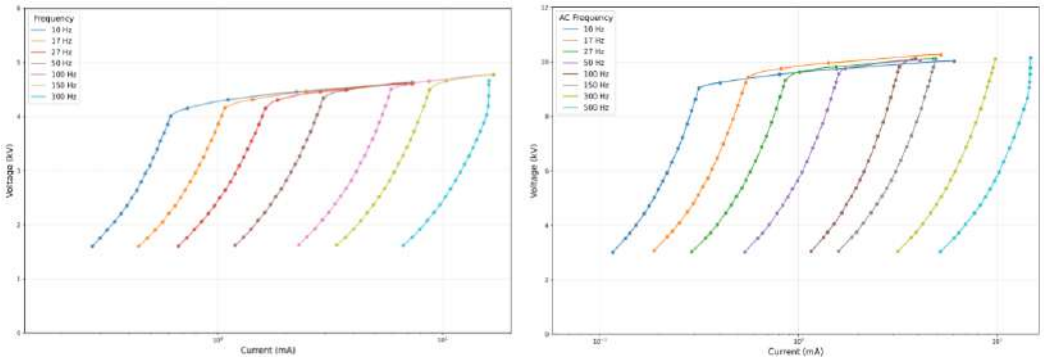

Figure 7. Measured V-I characteristics of the MOV blocks at different frequencies

4. Model Development

Based on the observed frequency-dependent behaviour, an RC network representation was developed for implementation in EMTP-ATP [5]. The model consists of three parallel RC branches, as shown in Figure 8, representing the distributed relaxation processes that occur within the arrester block at different frequencies, combined with a frequency-independent nonlinear resistor capturing the voltage-dependent conduction. The latter component has been extracted as part of the analysis done earlier. The choice of a three RC branch network is a tradeoff between the practical and accurate representation of the MOV grain boundary, sufficient for systems studies. The model, however, can be extended to more RC branches if a more accurate representation is needed.

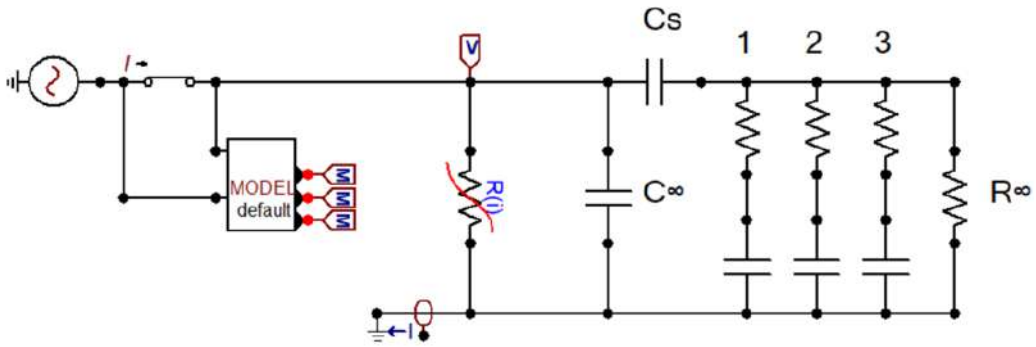

Figure 8. Frequency-dependent surge arrester model implemented in EMTP-ATP

Model parameters were obtained through a fitting process [6-7]. Table 2 presents the extracted RC network parameters for the first MOV block under testing and represents the following:

1. Each R_k-C_k branch represents one frequency decade of the block to capture the distributed nature of relaxation processes within the arrester grain boundary network.
2. C_∞ represents the capacitance of the arrester at any given frequency.
3. C_s blocks the dielectric loss circuit from contributing to the DC leakage current.
4. G_∞ sets the resistance limit of the circuit as frequency approaches zero.

Table 2. RC network parameters for the validation MOV model

Branch	C_k (nF)	R_k (MΩ)	External components:	
1	0.56	15.14	G_∞(R_∞)	0.831 nS (1203.9 MΩ)
2	0.22	3.85	C_∞	2 nF
3	0.11	0.77	C_s	2.5 nF

The frequency-dependent V-I characteristics of the model demonstrates the transition from capacitive behaviour at high frequencies to resistive behaviour at lower frequencies, as shown in Figure 9. The model reproduces the frequency ordering observed in measurements, with the current magnitude increasing as the frequency increases for a given voltage level. This behaviour directly impacts energy dissipation calculations for temporary overvoltages containing harmonic content.

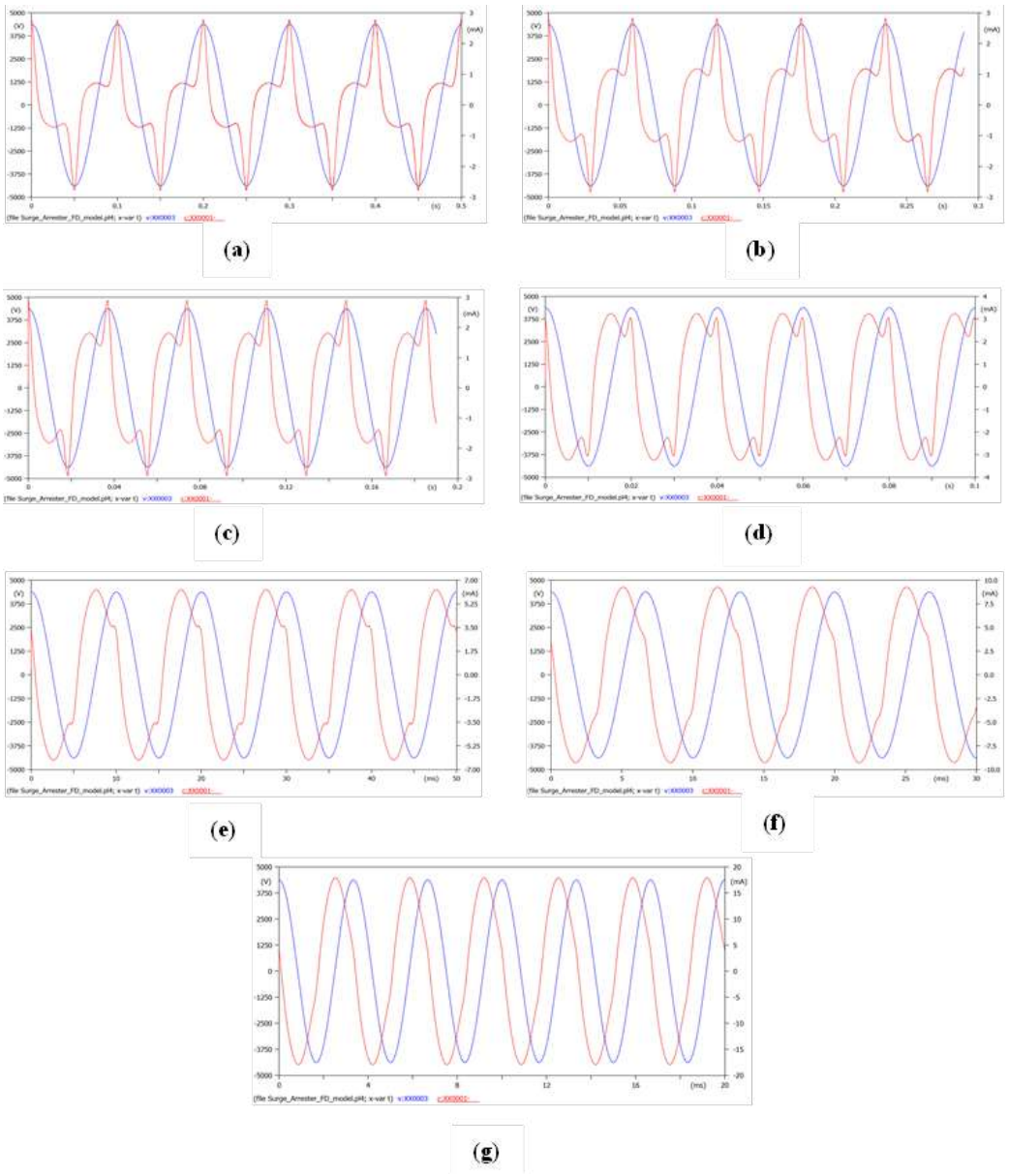

Figure 9. Frequency-dependent voltage-current characteristics of surge arrester model at 4.5 kV test voltage (a) 10 Hz (b) 17 Hz (c) 27 Hz (d) 50 Hz (e) 100 Hz (f) 150 Hz (g) 300 Hz

5. Model Validation

Model validations were done on both blocks, and more information can be found in [4]. Impedance validation was performed at 3 kV to evaluate the model's representation of frequency-dependent behaviour in the linear region. Figure 10 compares measured and modeled resistance and reactance components. The model reproduces the frequency-

dependent resistance within 15% error across the frequency range. Reactance agreement is within 10%, confirming an acceptable representation of the capacitive behaviour. The close tracking of both components validates the RC network's ability to represent the distributed impedance characteristics of the MOV block.

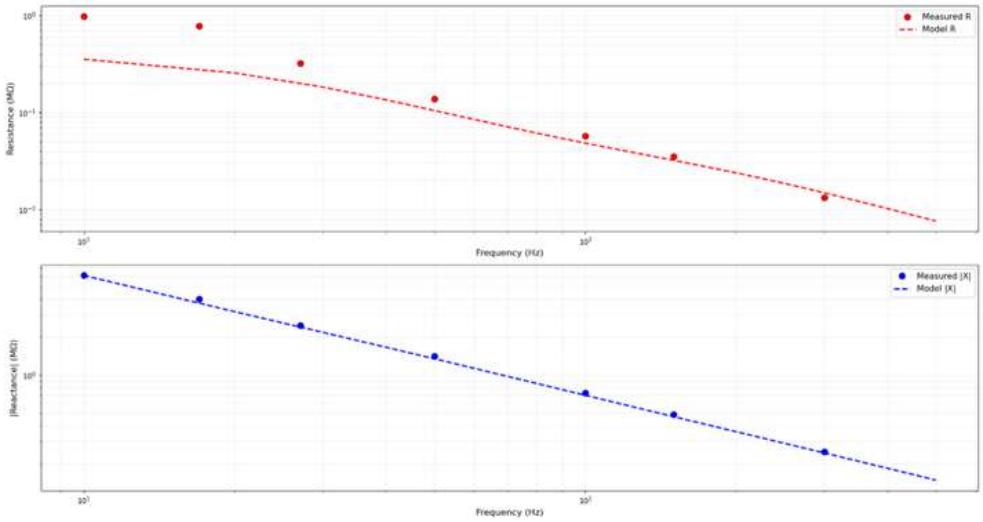

Figure 10. Impedance response validation at 3 kV: (a) resistance, (b) reactance

The validation of energy dissipation was performed across 42 test cases spanning seven frequencies and six voltage levels. Figure 11 presents the power losses and the cumulative energy compared between the measured MOV and the calculated FD model values for 3 test cases.

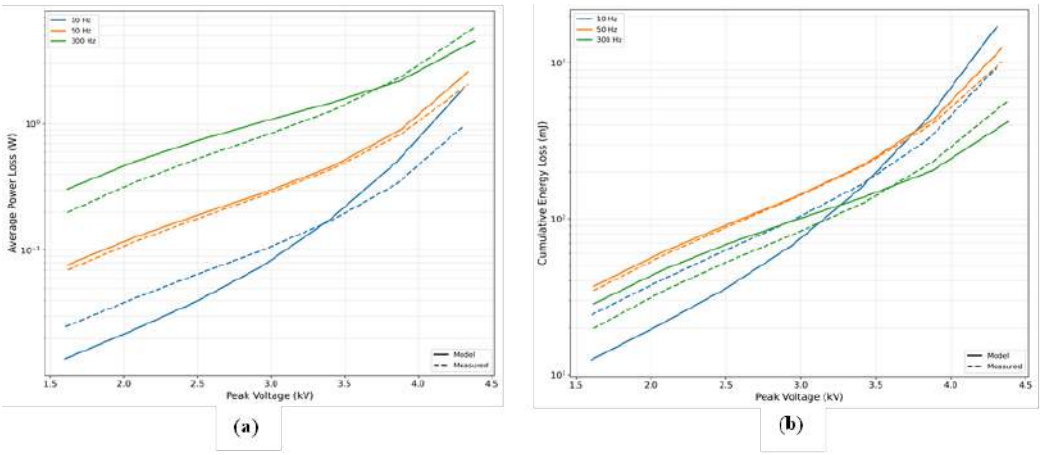

Figure 11. Comparison of measured and modeled energy dissipation parameters (a) Average power (b) Cumulative energy

The model maintains correct frequency ordering and captures the exponential voltage dependence across the tested range. Mean absolute errors are 22% for energy and 25% for

power, with best accuracy at 50 Hz where errors reduce below 10%. The systematic nature of the errors suggests that model accuracy could be improved through additional RC branches or optimizing it further, though the current three-branch implementation provides an adequate representation for engineering applications.

Direct comparison of measured and modeled V-I characteristics confirms the model's ability to represent the transition from linear to nonlinear conduction. Figure 12 shows this comparison across the tested frequency range. The model captures both the magnitude and slope of the V-I curves, indicating good representation of the voltage-dependent conduction mechanisms. Minor deviations at intermediate frequencies reflect the approximation inherent in representing a continuous relaxation spectrum with discrete RC branches.

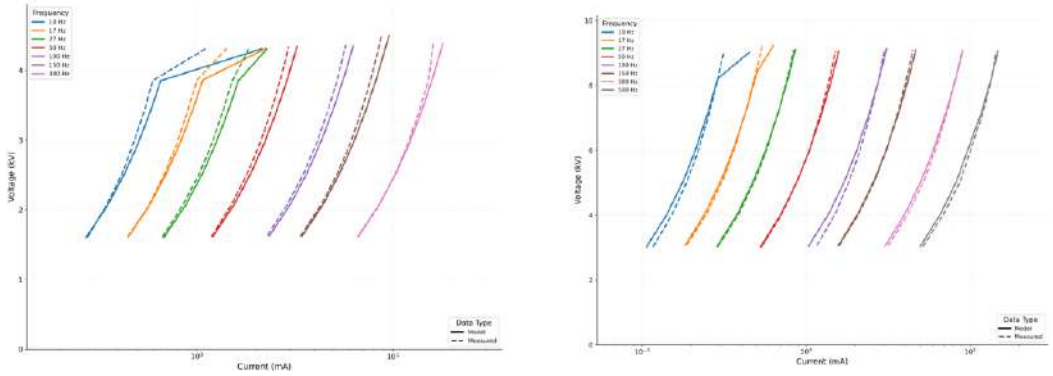

Figure 12. V-I characteristics: measured (solid) versus modeled (dashed) for first block (left) and second block (right)

6. Conclusions

A methodology has been developed to create a frequency-dependent model for surge arresters based on impedance measurements across multiple frequencies. The experimental work demonstrated that the arrester capacitance remains frequency-independent, while the resistance decreases significantly with increasing frequency. This frequency-dependent resistance represents dielectric losses in the grain boundary network and substantially affects the energy dissipation under harmonic TOV conditions.

The RC network model implemented in EMTP-ATP reproduces the measured behavior within engineering-acceptable accuracy. The model maintains correct frequency ordering and captures the exponential voltage dependence required for insulation coordination studies. A pipeline framework for automated parameter extraction through differential evolution has been developed, enabling possible adaptation to different MOV blocks without manual adjustment and, thus, making the methodology suitable for industry applications.

The energy dissipation at harmonic frequencies varies substantially from power-frequency predictions. This variation becomes unavoidable when assessing surge arrester performance in cable-rich networks where harmonic resonances could be excited during transformer energization and other system disturbances. Therefore, the frequency-dependent model provides a practical tool for assessing surge arrester performance under realistic grid conditions where harmonic content cannot be neglected. This work will continue by:

1. Implementing optimization frameworks for automated parameter extraction, potentially employing machine learning techniques.
2. Extension of the MOV block model to a full surge arrester model and validation based on system studies.
3. Integrating temperature-dependent behaviour and hysteresis effects of the MOV block into the frequency-dependent model.
4. Investigating how ageing mechanisms impact frequency-dependent behaviour by tracking impedance changes across the frequency spectrum over time

References

[1] CIGRE Technical Brochure 913, Evaluation of Temporary Overvoltages in Power Systems due to Low Order Harmonic Resonances, 2023

[2] K. Velitsikakis, I. Tannemaat, Surge Arrester Stresses due to Harmonic Resonance Temporary Overvoltages in Transmission Systems: A Case Study of the Dutch Grid, INMR World Congress, Berlin, 2022

[3] IEC 60071-4, Insulation Co-ordination – Part 4: Computational Guide to Insulation Co-ordination and Modelling of Electrical Networks, 2004

[4] S.P.P. Dhulipala, Characterization of Arresters for Harmonic Overvoltage Studies, Delft University of Technology, August 2025

[5] https://atp-emtp.org/index.php

[6] K. Kundert, Modeling Dielectric Absorption in Capacitors, 2021

[7] A. Oustaloup, F. Levron, B. Mathieu, F.M. Nanot, Frequency-band Complex Noninteger Differentiator: Characterization and Synthesis, IEEE Transactions on Circuits and Systems I: Fundamental Theory and Applications, Vol. 47, Issue 1, 2000